



AFRL-RY-HS-TR-2010-0012

Similarity Scaling for the Inner Region of the Turbulent Boundary Layer

David W. Weyburne

AFRL/RYHC
80 Scott Drive
Hanscom AFB, MA 01731-2909

20 November 2009

In-House Technical Report

APPROVED FOR PUBLIC RELEASE; DISTRIBUTION UNLIMITED

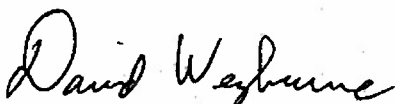
AIR FORCE RESEARCH LABORATORY
Sensors Directorate
Electromagnetics Technology Division
Hanscom AFB MA 01731-2909

NOTICE AND SIGNATURE PAGE

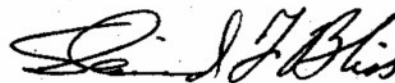
Using Government drawings, specifications, or other data included in this document for any purpose other than Government procurement does not in any way obligate the U.S. Government. The fact that the Government formulated or supplied the drawings, specifications, or other data does not license the holder or any other person or corporation; or convey any rights or permission to manufacture, use, or sell any patented invention that may relate to them.

This report was cleared for public release by the Electronic Systems Center Public Affairs Office for the Air Force Research Laboratory Electromagnetic Technology Division and is available to the general public, including foreign nationals. Copies may be obtained from the Defense Technical Information Center (DTIC) (<http://www.dtic.mil>).

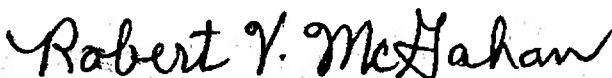
AFRL-RY-HS-TR-2010-0012 HAS BEEN REVIEWED AND IS APPROVED FOR PUBLICATION IN ACCORDANCE WITH ASSIGNED DISTRIBUTION STATEMENT.



DAVID WEYBURN
Contract Monitor



DAVID F. BLISS, Acting Chief
Optoelectronic Technology Branch



DR. ROBERT V. McGAHAN
Technical Communications Advisor
Electromagnetics Technology Division

This report is published in the interest of scientific and technical information exchange, and its publication does not constitute the Government's approval or disapproval of its ideas or findings.

REPORT DOCUMENTATION PAGE			Form Approved OMB No. 0704-0188	
Public reporting burden for this collection of information is estimated to average 1 hour per response, including the time for reviewing instructions, searching existing data sources, gathering and maintaining the data needed, and completing and reviewing this collection of information. Send comments regarding this burden estimate or any other aspect of this collection of information, including suggestions for reducing this burden to Department of Defense, Washington Headquarters Services, Directorate for Information Operations and Reports (0704-0188), 1215 Jefferson Davis Highway, Suite 1204, Arlington, VA 22202-4302. Respondents should be aware that notwithstanding any other provision of law, no person shall be subject to any penalty for failing to comply with a collection of information if it does not display a currently valid OMB control number. PLEASE DO NOT RETURN YOUR FORM TO THE ABOVE ADDRESS.				
1. REPORT DATE (DD-MM-YYYY) 11-20-2009		2. REPORT TYPE Technical Report		3. DATES COVERED (From - To) 1 Dec 2008 – 1 Sep 2009
4. TITLE AND SUBTITLE Similarity Scaling for the Inner Region of the Turbulent Boundary Layer		5a. CONTRACT NUMBER In-House		
		5b. GRANT NUMBER		
		5c. PROGRAM ELEMENT NUMBER 624916		
6. AUTHOR(S) David W. Weyburne		5d. PROJECT NUMBER 4916		
		5e. TASK NUMBER HC		
		5f. WORK UNIT NUMBER 01		
7. PERFORMING ORGANIZATION NAME(S) AND ADDRESS(ES) AFRL/RYHC 80 Scott Drive Hanscom AFB, MA 01731-2909		8. PERFORMING ORGANIZATION REPORT NUMBER		
9. SPONSORING / MONITORING AGENCY NAME(S) AND ADDRESS(ES) Electromagnetics Technology Division Sensors Directorate Air Force Research Laboratory 80 Scott Drive Hanscom AFB, MA 01731-2909 Source Code:437890		10. SPONSOR/MONITOR'S ACRONYM(S) AFRL/RYHC		
		11. SPONSOR/MONITOR'S REPORT NUMBER(S) AFRL-RY-HS-TR-2010-0012		
12. DISTRIBUTION / AVAILABILITY STATEMENT DISTRIBUTION A: APPROVED FOR PUBLIC RELEASE: DISTRIBUTION UNLIMITED				
13. SUPPLEMENTARY NOTES The U.S. Government is joint author of this work and has the right to use, modify, reproduce, release, perform, display, or disclose the work. Cleared for Public Release by 66 ABW-2010-0074, 25 January 2010.				
14. ABSTRACT For the first time it is shown that the Prandtl length scale has a natural interpretation in terms of the physical structure of the boundary layer for a 2-D wall bounded flow. Both the Prandtl length scale and a newly developed parameter are first moments associated with the mean location value of the second derivative of the velocity profile. These two parameters therefore track the mean location of the viscous forces present in the boundary layer. A simple mathematical proof is offered to show that the new parameter must be a similarity scaling parameter for all 2-D boundary layer flows. From the parameter definitions, one can show that the new scaling parameter is identical to the Prandtl parameter scaling for the case where the ratio of the free stream velocity at the boundary layer edge to the Prandtl scaling velocity, the so called friction velocity, is a constant. This similarity condition is found in certain turbulent boundary layer flow data sets. We show that to experimental accuracy, a subset of these datasets exhibit whole profile similarity using the new scaling parameters if one assumes that the reported skin friction coefficients are in error by $\pm 10\%$. The results lead to a new conceptual picture for similarity of the turbulent boundary layer.				
15. SUBJECT TERMS Fluid Boundary Layers, Velocity Profiles, Turbulent Flow, Inner layer Region, Similarity Scaling				
16. SECURITY CLASSIFICATION OF:			17. LIMITATION OF ABSTRACT	18. NUMBER OF PAGES
a. REPORT Unclassified	b. ABSTRACT Unclassified	c. THIS PAGE Unclassified	SAR	36
				19a. NAME OF RESPONSIBLE PERSON David W. Weyburne
				19b. TELEPHONE NUMBER n/a

Contents

List of Figures	iv
Acknowledgments	vi
Summary	1
1. Introduction	2
2. Second Derivative Moments	3
2.1 Boundary Layer Edge Moments	4
2.2 Boundary Layer Wall Moments	5
3. The Mathematics of Similarity	7
3.1 Velocity Profile Scaling	7
3.2 First Derivative Profile Scaling	8
3.3 Second Derivative Profile Scaling	9
3.4 Prandtl Similarity Scaling	9
4. New Scaling versus Prandtl Scaling	10
4.1 Laminar Flow Similarity	10
4.2 Inner Region Turbulent Flow Similarity	11
4.3 Whole Profile Turbulent Flow Similarity	13
5. Conceptualizing the Turbulent Boundary Layer	16
5.1 <i>Current Scaling Model</i>	16
5.2 <i>New Scaling Model</i>	17
6. Discussion	20
7. Conclusion	23
8. References	24

List of Figures

Figure 1. The black line is the second derivative of the Blasius [17] solution for laminar flow using the Schlichting [18] tabulated values.	4
Figure 2. The black line is the ZPG DNS results from Khujadze and Oberlack [19] with $Re_\theta=2807.098$	4
Figure 3a. DeGraaff and Eaton [5] velocity profiles taken at $Re_\theta=1430, 2900$, and 5200 using μ_1 and u_e scaling.	12
Figure 3b. DeGraaff and Eaton [5] velocity profiles taken at $Re_\theta=1430, 2900$, and 5200 using Prandtl plus scaling.	12
Figure 4a. Five Österlund [21] velocity profiles with $u_e \cong 10.3$ m/s consisting of SW981129A, SW981128A, SW981127H, SW981126C, and SW981112A datasets using μ_1 and u_e scaling.	12
Figure 4b. Five Österlund [21] velocity profiles with $u_e \cong 10.3$ m/s consisting of SW981129A, SW981128A, SW981127H, SW981126C, and SW981112A datasets using Prandtl plus scaling.	12
Figure 5a. Seven velocity profiles from Skåre and Krogstad [22] using μ_1 and u_e scaling.	13
Figure 5b. Seven velocity profiles from Skåre and Krogstad [22] using Prandtl plus scaling.	13
Figure 6a. The seven full scale velocity profiles from Skåre and Krogstad [22] using μ_1 and u_e scaling.	14
Figure 6b. The seven full scale velocity profiles from Skåre and Krogstad [22] using Prandtl plus scaling.	14
Figure 7. The seven full scale velocity profiles from Skåre and Krogstad [22] using δ_1 and u_e scaling.	14
Figure 8. A reproduction of Skåre and Krogstad's [22] Fig. 4a showing their reported c_f data along with the inferred c_f data.	15
Figure 9. The seven velocity profiles (black lines) from Skåre and Krogstad [22] using the inferred c_f data to calculate μ_1	15

Figure 10a. Ten profiles from Schubauer and Klebanoff [32] using the scaled defect profile for the y-axis.	19
Figure 10b. Ten profiles from Schubauer and Klebanoff [32] using the scaled velocity profile for the y-axis.	19
Figure 11. The ZPG DNS results (+) from Khujadze and Oberlack [19] with $R_\theta=2807.098$. The red line is the Log Law.	21

Acknowledgement

The author would like to acknowledge the support of the Electromagnetics Technology Division of the Sensors Directorate of the Air Force Research Laboratory. In addition, the author would like to thank a number of authors who contributed their experimental datasets including David DeGraaff and John Eaton, George Khujadze and Martin Oberlack, Jens Österlund, and Per Egil Skåre and Per-Åge Krogstad.

Summary For the first time it is shown that the Prandtl length scale has a natural interpretation in terms of the physical structure of the boundary layer for a 2-D wall bounded flow. The Prandtl length scale is closely related to a new length scale parameter μ_1 that was developed to describe 2-D wall bounded flows using the method of integral moments. Both the Prandtl length scale and the new parameter μ_1 are first moments associated with the mean location value of the second derivative of the velocity profile. These two parameters therefore track the mean location of the viscous forces present in the boundary layer. A simple mathematical proof is offered to show that if similarity exists in a set of velocity profiles, then μ_1 must be a similarity scaling parameter. The associated velocity scaling variable is the free stream velocity. In contrast, we show that for laminar flow over a wedge, the more familiar Prandtl scalings are not similarity scaling parameters. And yet for the viscous region of turbulent flows, it appears that the Prandtl scaling is better at tracking the viscous forces than μ_1 . As one goes deeper into the boundary layer, into the Logarithmic Law region, experimental results continue to favor the Prandtl scalings over μ_1 in terms of similarity. The explanation for this comes from the fact that μ_1 is defined in terms of inner and outer parameters whereas the Prandtl scaling are defined using inner scaling only. From the parameter definitions, one can show that μ_1 is identical to the Prandtl parameter scaling for the case where the ratio of the free stream velocity at the boundary layer edge to the Prandtl scaling velocity, the so called friction velocity, is a constant. This Rotta similarity condition is found to hold in certain turbulent boundary layer flow data sets. We show that to experimental accuracy, a subset of these datasets exhibit whole profile similarity using the μ_1 scaling parameter if one assumes that the reported skin friction coefficients are in error by $\pm 10\%$. The results lead to a new conceptual picture for similarity of the turbulent boundary layer.

1. Introduction

Beginning with the pioneering work of Reynolds [1], there has been a concerted effort to find coordinate scaling parameters that make the scaled velocity profiles and shear-stress profiles taken at different stations along the flow appear to be nearly identical. For turbulent boundary layers, this search for “similarity” was mostly unsuccessful. This led to the practice of dividing the turbulent profile into two regions, an inner region dominated by viscous forces and outer region dominated by turbulent inertial forces. It has been universally accepted that the Prandtl [2] scaling parameters are the correct scaling form for the turbulent boundary layers inner region [3]. The main reason for this would seem to be that the Prandtl scaling parameters in the form of the Logarithmic Law (Log Law for short) have been successful at producing similar velocity profiles in the Log Law region for a wide range of experimental datasets. The Log Law applies to the overlap region between the inner and outer regions and states that in this overlap region of the turbulent boundary layer, the velocity in the streamwise x -direction $u(x, y)$ is given by

$$\frac{u(x, y)}{u_\tau} = \frac{1}{\kappa} \ln \left(\frac{yu_\tau}{\nu} \right) + B \quad (1)$$

where y is the height perpendicular to the solid surface, ν is kinematic viscosity, κ and B are constants, and u_τ is the Prandtl velocity scaling parameter, the so-called friction velocity.

Although there is an ongoing controversy as to the universality of the Log Law, experimental results indicate that the Log Law is widely applicable to most turbulent boundary layer flows (see for example Monkewitz, Chauhan, and Nagib [4]). However, the Log Law region does not extend to the wall. Recently, there have been a number of papers [5-9] that indicate that experimental evidence supports the use of the Prandtl scaling all the way to wall.

The experimental evidence for the Prandtl scaling is very strong for the inner region of the turbulent boundary layer. However, it must be acknowledged that the Prandtl length scale ν/u_τ is not what one would consider a normal length parameter. There have been a few studies that have tried to introduce alternative length scales for the inner layer region. For example, Bushmann and Gad-el-Hak [10] have pointed out that the Zagarola and Smits [11] velocity scaling works as well as the Prandtl scaling for the inner region of certain turbulent channel flows, turbulent pipe flows, and the Zero Pressure Gradient (ZPG) turbulent boundary layer flows. Recently, Weyburne [12,13] introduced a way of describing the thickness and shape of the boundary layer velocity profiles using the standard moment method that is normally used to describe probability density functions (PDFs). These new parameters were developed from the observation that for laminar flow over a flat plate, the second derivative of the stream-wise velocity $u(x, y)$ in the y -direction (normal to the plate) has a very Gaussian-like profile [12]. Borrowing from probability density function methodology, the boundary layer was then described in terms of the central moments of this Gaussian-like kernel. The most important result of this approach is that for the first time, we have a mathematically well-defined way to describe the viscous boundary layer thickness and shape.

Although first applied to laminar flow, it is self-evident that these second derivative moments should track the thickness and shape of the inner viscous region for the wall-bounded turbulent boundary layer as well. One of these parameters is the mean location of the second derivative profile μ_1 given by

$$\frac{u_e}{\mu_1} = \frac{du(x, y)}{dy} \Big|_{y=0} \quad (2)$$

where u_e is the value of $u(x, y)$ at the boundary layer edge. Technically, this mean location should work for laminar and turbulent boundary layers. However, in what follows, we use the moment method to show that for the turbulent boundary layer, the mean location of the second derivative profile is better tracked by the Prandtl length scale ν/u_τ rather than μ_1 . This means that for the first time it is possible to show that the Prandtl length scale ν/u_τ has an interpretation that can be traced back to the physical structure of the boundary layer.

A major advantage of the scaling parameter μ_1 is that it can be shown mathematically that for flows showing similarity over the whole velocity profile, then μ_1 must be a similarity length scaling parameter. This result is a follow-up to an earlier result in which Weyburne [14] presented a mathematical proof showing that for flows that show outer layer similarity, the displacement thickness δ_1 and u_e must be similarity scaling parameters. In what follows, we show that μ_1 must also be a similarity scaling parameter and that under special circumstances the Prandtl scale ν/u_τ is also a similarity scaling parameter.

For laminar flow on a wedge we show that μ_1 is a similarity length scaling constant and that the Prandtl length scale is not. For turbulent boundary layer, the picture is more complicated. As already discussed above and as will be demonstrated below, experimental results definitely favors the Prandtl parameter scaling over the μ_1 scaling in terms of similarity scaling of the inner region of the turbulent velocity profile. And yet the first principles mathematical proof offered herein indicates that for similarity over the whole profile, the scaling must be the new scaling given by μ_1 and u_e . This dichotomy is explained by the observation that turbulent boundary layers in general do not show whole profile similarity. Thus it would appear that for similarity, the new scaling is limited to laminar flow situations. However, we show that μ_1 is equivalent to the Prandtl length scale ν/u_τ for the case where the ratio u_e/u_τ is a constant. This Rotta [15] similarity condition is found in certain turbulent boundary layer flow datasets. In what follows, we show that to experimental accuracy, a subset of these datasets exhibit whole profile similarity using the new scaling parameters if one assumes that the reported skin friction coefficients are in error by $\pm 10\%$.

The new results presented herein together with earlier results for outer layer similarity [16] allow us to develop a new conceptual model of similarity of the turbulent boundary layer that is very different then the present conceptual model. We begin by first briefly introducing the relevant mathematical equations for describing the inner layer region of the turbulent boundary layer.

2. Second Derivative Moments

In an earlier paper, Weyburne [12,13] employed the moment methodology normally used to describe probability density functions (PDFs) in order to describe the thickness and shape of a 2-D boundary layer. In the next section below we briefly review this formulation. This formulation was based on using the outer layer normalizing velocity u_e . We follow this with a

moment development that uses the Prandtl scaling velocity u_τ as the normalizing velocity. In order to differentiate the two moment developments, we will use the term “edge” moments and “wall” moments.

2.1 Boundary Layer Edge Moments

In this Section, we briefly review the equations and parameters developed by Weyburne [12,13]. The original derivation was based on the observation that the second derivative of the laminar velocity profile had a Gaussian-like appearance as illustrated in Fig. 1. In this figure we show the Blasius [17] solution for laminar flow on a flat plate. For comparison purposes, we plot a sample Direct Numerical Simulation [19] calculation of a turbulent boundary layer on a flat plate in Fig. 2. Notice that in this case, the plotted profile has a skewed Gaussian-like appearance.

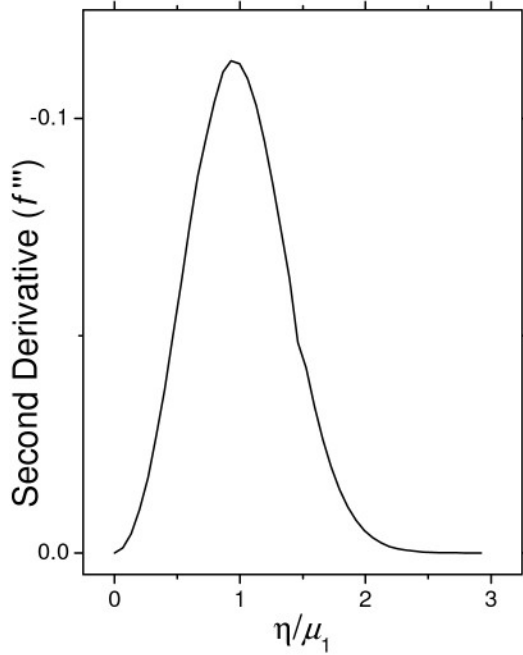


Figure 1: Blasius [17] solution for laminar flow using the tabulated data from Schlitching [18].

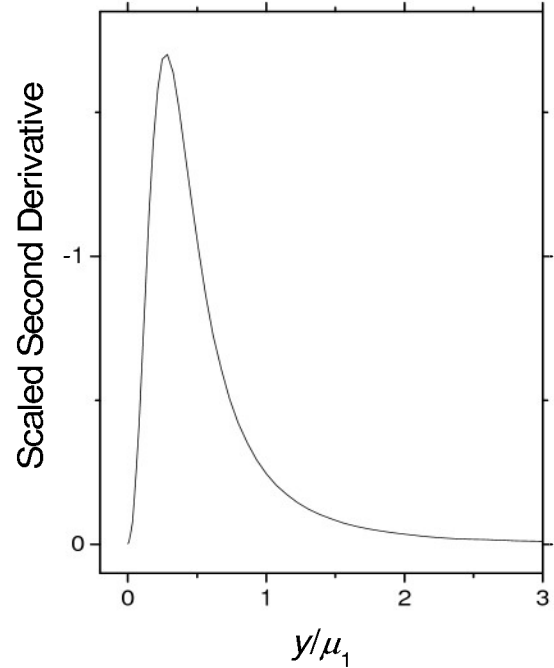


Figure 2: The DNS solution for the ZPG turbulent boundary layer from Khujadze and Oberlack [19].

The standard method for describing PDFs like the Gaussian curve is to use the method of central moments. It follows, therefore, that laminar boundary layer flow and the viscous sublayer of a turbulent boundary layer can be characterized by moments of the second derivative profile just as one uses moments to describe PDFs. The moment description of the viscous layer starts by introducing the viscous velocity boundary layer n th central moment λ_n given by

$$\lambda_n \equiv \int_0^h dy (y - \mu_1)^n \frac{d^2 \{-\mu_1 u(x, y)/u_e\}}{dy^2} \quad , \quad (3)$$

where h is located deep into the free stream, and where μ_1 is the first moment about the origin. The moments about the origin are given by

$$\mu_n \equiv \int_0^h dy y^n \frac{d^2 \{-\mu_1 u(x, y)/u_e\}}{dy^2} . \quad (4)$$

The numerator of the derivatives in Eqs. 3 and 4 are written in this way to emphasize the PDF-like appearance of this second derivative term. The mean location of the second derivative of the velocity relative to the boundary layer edge is μ_1 and is actually defined by the requirement that $\lambda_0 = \mu_0 = 1$ which is how Eq. 2 is derived.

The second central moment is related to a parameter we call the viscous boundary layer width given by $\sigma_v = \sqrt{\lambda_2}$. The physical description of the shape of the viscous boundary layer is extended by using the third and fourth moments to define the viscous boundary layer skewness $\gamma_1 = \lambda_3 / \sigma_v^3$ and the viscous boundary layer excess $\gamma_2 = \lambda_4 / \sigma_v^4 - 3$. Notice that the turbulent flow curve (Fig. 2) is noticeably skewed compared to the laminar flow profile (Fig. 1). This fact is emphasized by looking at the skewness parameter γ_1 . For laminar flow (Fig. 1), the skewness value is $\gamma_1 = 0.3$ whereas for the turbulent flow curve (Fig. 2), the value is $\gamma_1 = 7.8$ (this value is for this profile but will change from one profile to the next). For comparison, the skewness of a Gaussian curve is $\gamma_1 = 0$.

It should be emphasized that the second derivative moments are only part of the moment based description of the boundary layer shape and thickness [13]. In addition to the second derivative moments, it is also straightforward to describe parameters based on the first derivative profile and the velocity profile itself. This allows one to track the viscous region as well as the outer region using the appropriate parameters.

2.2 Boundary Layer Wall Moments

Notice that Weyburne's original description used the boundary layer edge velocity u_e to normalize the velocity. It is possible to use the friction velocity u_τ instead. Thus we can define a viscous velocity boundary layer n th wall moment ζ_n as

$$\zeta_n \equiv \int_0^h dy (y - \omega_1)^n \frac{d^2 \{-\alpha_1 u(x, y)/u_\tau\}}{dy^2} , \quad (5)$$

where " $-\alpha_1$ " term in the derivative's numerator is there as a normalizing parameter, and where ω_1 term is the mean viscous location of the wall moments about the origin defined as

$$\omega_n \equiv \int_0^h dy y^n \frac{d^2 \{-\alpha_1 u(x, y)/u_\tau\}}{dy^2} . \quad (6)$$

The value of the normalizing parameter α_1 can be found by noting that the zeroth moments are defined by $\omega_0 = \zeta_0 = 1$ so that

$$1 \equiv \int_0^h dy \frac{d^2 \{-\alpha_1 u(x, y)/u_\tau\}}{dy^2} \Rightarrow \frac{u_\tau}{\alpha_1} = \frac{du(x, y)}{dy} \Big|_{y=0} \quad (7)$$

Since the friction velocity is defined as

$$u_\tau = \sqrt{\frac{\tau_w}{\rho}} = \sqrt{\nu \left(\frac{du(x, y)}{dy} \right)_{y=0}}, \quad (8)$$

where τ_w is the wall shear stress, then it easy to show that

$$\alpha_1 = \frac{\nu}{u_\tau}. \quad (9)$$

The mean location of the second derivative at the wall then reduces to

$$\omega_1 = \int_0^h dy y \frac{d^2 \left\{ -\frac{\nu u(x, y)}{u_\tau^2} \right\}}{dy^2} \quad (10)$$

Integrating Eq. 10 by parts, it is easily shown that $\omega_1 = \mu_1$ if one takes $y = h$ to be deep into the free stream. This is to be expected. The wall moments (Eqs. 5-6) and the edge moments (Eqs. 3-4) should be independent of the velocity normalizing constant and result in the same moment values.

This result, while technically correct, has a problem. We know that the viscous region for the turbulent boundary layer is confined to the very near wall region yet our integral limit is taken at the outer boundary layer edge. Let us reconsider Eq. 10. After integrating by parts, this equation reduces to

$$\omega_1 = \left\{ \frac{\nu}{u_\tau} \frac{u(x, y)}{u_\tau} \right\}_{y=h,0}. \quad (11)$$

If one takes $y=h$, where h is deep into the free stream then this reduces to $\omega_1 = \mu_1$ as already noted. However, from decades of experimental work we know that the viscous region, and hence the second derivative profile is only numerically significant in a region from $y=0$ to about $y \cong 70\nu/u_\tau$ (for comparison, the boundary layer edge is located at about $y \cong 1070\nu/u_\tau$). For the DNS example used in Fig. 2, we note that the second derivative value falls to a value less than 1% of the peak height at $y \cong 70\nu/u_\tau$. If we take $h = 70\nu/u_\tau$ in Eq. 11, then for the turbulent boundary layer we have $u(x, h) \cong 15u_\tau$. The exact numerical value will dependent on the pressure gradient and Reynolds number but is approximately correct. This means that for the turbulent boundary layer, the mean location of the second derivative profile is given by

$$\omega_1 \cong 15 \frac{\nu}{u_\tau}. \quad (12)$$

What is important here is that as far as scaling for the turbulent boundary layer is concerned, the mean location is directly proportional to the Prandtl length scale! Therefore, this result indicates that the Prandtl length scale is tracking the viscous forces of the turbulent boundary layer. This result explains the reason the Prandtl length scale has been so successful at scaling the inner region of the turbulent boundary layer.

3. The Mathematics of Similarity

Now that μ_1 and ν/u_τ have been properly defined, we turn to the task of looking at the theoretical aspects of velocity profile scaling. We start by reproducing some of the results from Weyburne [14] in regards to similarity scaling. We then extend the earlier work to the scaled second derivative profile in order to obtain new similarity results.

3.1 Velocity Profile Similarity

In the earlier paper by Weyburne[14], a first principles mathematical proof for the existence of certain length and velocity scales was obtained for the similarity scaling of 2-D wall-bounded flows. The proof is based on a simple concept; the area under similar scaled velocity profile curves must be equal. By taking certain integrals of the scaled velocity profiles and its first derivative, a number of similarity scaling requirements were obtained. The analysis is reproduced below.

It is important to point out that in the analysis below, no assumptions are necessary as to the functional form of the velocity profile $u(x,y)$. The only requirements are that the boundary conditions for the velocity profile are known. Consider a 2-D flow along a body such that the y -direction is normal to the body's surface. We start by defining a length scaling parameter $\delta(x)$ and a velocity scaling parameter $u_s(x)$. The length and velocity scaling variables $\delta(x)$ and $u_s(x)$ can vary with the flow direction (x -direction) but not in the y -direction. Starting with the formal definition of similarity, that is two velocity profiles are similar if they differ only by a scaling constant in y and $u(x,y)$ for all y -values, then it is self evident that for two profiles to be similar, the area under the properly scaled velocity profiles must be equal. The area under the scaled profiles, in mathematical terms, is given by

$$c(x) = \int_0^{h/\delta(x)} d\left\{\frac{y}{\delta(x)}\right\} \{u_e - u(x,y)\}/u_s(x) \quad , \quad (13)$$

where $c(x)$ is a nonzero numerical constant, and $y=h$ is deep into the free stream. The integral is written using the velocity difference so that the integral value is not dependent on the numerical value of h as long as h is located deep in the free stream. Using a variable switch ($d\{y/\delta\} \Rightarrow (1/\delta)dy$) and simple algebra, it is easily verified that Eq. 13 reduces to

$$c(x) = \frac{u_e \delta_1}{u_s(x) \delta(x)} \quad , \quad (14)$$

where the δ_1 is the displacement thickness given by

$$\delta_1 \equiv \int_0^h dy \{1 - u(x,y)/u_e\} \quad . \quad (15)$$

Eq. 14 is an exact equation that applies whether the profiles are similar or not. A necessary, but not sufficient, condition for similarity is that the $c(x)$ values for each profile of the set of profiles being tested are equal. If the profiles are similar, then for scaling purposes, one can take $c(x)=1$ in Eq. 14. This equation then becomes the empirically derived velocity scale successfully used by Zagarola and Smits [11] to scale turbulent boundary flows over wedges, in channels, and in pipes. The importance of Eq. 14 in regards to similar profiles is that it means that the thickness scaling and the velocity scaling variables are not independent for 2-D wall bounded similarity flows.

3.2. First Derivative Profile Scaling

By considering the area under the velocity profiles we were able to establish the interdependence of the length and velocity scaling. We can make additional derivations using the same methodology from above. We now extend the mathematics of similarity to the first derivative profiles and find additional similarity requirements. If similarity is present in a set of scaled velocity profiles then it is self evident that the scaled first derivative profiles (derivative with respect to the scaled y -coordinate) must also be similar. It is also self evident that the area under the scaled first derivative profiles must be equal for similarity. Furthermore, the area under the scaled first derivative profiles times the scaled y -coordinate to the power one must also be equal for similarity to exist.

In mathematical terms, equal area under the scaled first derivative profiles is expressed by

$$b(x) \equiv - \int_0^{h/\delta(x)} d\left\{\frac{y}{\delta(x)}\right\} \frac{d\{u_e - u(x, y)\}/u_s(x)}{d\left\{\frac{y}{\delta(x)}\right\}}, \quad (16)$$

where $b(x)$ is a non-zero numerical constant. Using the boundary conditions $u(x, 0)=0$ and $u(x, h)=u_e$ combined with a simple variable switch, then by inspection one sees that Eq. 16 reduces to

$$b(x) = \frac{u_e}{u_s(x)}. \quad (17)$$

For similarity of the velocity profiles in this geometry, we must have $b(x)$ equal to a non-zero constant. This means that for similar velocity profiles, the scaling velocity must be a constant proportional to the free stream velocity at the boundary layer edge u_e .

Next, in mathematical terms, having equal area under the scaled first derivative profiles times the scaled y -coordinate (to the power one) is equivalent to

$$d(x) = \int_0^{h/\delta(x)} d\left\{\frac{y}{\delta(x)}\right\} \frac{y}{\delta(x)} \frac{d\{u(x, y)/u_e\}}{d\left\{\frac{y}{\delta(x)}\right\}}, \quad (18)$$

where $d(x)$ is a non-zero numerical constant. After a simple variable switch and integration by parts, it is easily verified that this equation reduces to

$$d(x) = \delta_1 / \delta(x). \quad (19)$$

Eq. 19 is important in that it states that if similarity exists, *i.e.* if $d(x)$ is a non-zero constant for a range of x -values, then the displacement thickness must be a length scale that results in similarity for both the velocity profiles and the first derivative profiles. Therefore, using simple mathematics, we have determined that the displacement thickness δ_1 must be similarity length scaling variable if similarity is found to exist in a set of velocity profiles. From Eq. 17, we also know that u_e must be a similarity velocity scaling variable for 2-D wall bounded flows.

3.3 The Second Derivative Profile

The above scaling results were obtained in the earlier paper [14]. Using the same methodology from above, we can extend the mathematics of similarity to the second derivative profile and find additional similarity requirements for the velocity profile. If similarity is present in a set of scaled velocity profiles then it is self evident that the scaled second derivative profiles (derivative with respect to y) must also be similar. It is also self evident that the area under the scaled second derivative profiles must be equal for similarity.

In mathematical terms, this is expressed by the following. We start by using the scaling constants from above that were discovered to work for 2-D wall bounded flows. Thus, δ_1 will be used to scale the y -variable and u_e to scale the velocity. The similarity requirement for equal area under the scaled second derivative profiles is therefore

$$a(x) = \int_0^{h/\delta_1} d\left\{\frac{y}{\delta_1}\right\} \frac{d^2\{u(x, y)/u_e\}}{d\left\{\frac{y}{\delta_1}\right\}^2} , \quad (20)$$

where $a(x)$ is a non-zero numerical constant. Using the definition of the mean location of the second derivative profile μ_1 given by Eq. 2, it is easily verified that Eq. 20 reduces to

$$a(x) = \frac{\delta_1}{\mu_1} . \quad (21)$$

Eq. 21 indicates that if similarity exists in a set of velocity profiles ($a(x)=\text{constant}$), then μ_1 must be a similarity length scale variable. From Eq. 17, we also know that if similarity exists in a set of velocity profiles, then u_e must be a similarity velocity scaling variable for 2-D wall bounded flows.

3.4. Prandtl Similarity Scaling

If similarity exists in a set of velocity profiles for 2-D boundary layer flows, then δ_1 , μ_1 , and u_e must be similarity scaling parameters. The question becomes what can be said about the Prandtl scaling parameters. Using Eqs. 2 and 8, it is evident that the ratio of the new scaling parameter μ_1 to the Prandtl scaling parameter ν/u_τ will be a constant if

$$\frac{u_e}{u_\tau} = \text{constant} . \quad (22)$$

This is of course the Rotta [15] condition for similarity of the turbulent boundary layer. If the Rotta condition holds, then either the Prandtl scaling parameters or the μ_1 and u_e scaling must work equally well since they will be equivalent.

4. Similarity Scaling

So far we have shown that the μ_1 scaling and the Prandtl ν/u_τ scaling have a solid physical basis. From first principles, we have also established that the new inner layer scaling parameter μ_1 is a similarity constant if similarity exists in a set of velocity profiles and that the Prandtl scaling parameters will also work if the Rotta condition (Eq. 22) holds. Now we turn to the question of whether the new parameters work as an inner region scaling parameter in real fluids. We start by considering laminar flow.

4.1 Laminar Flow Similarity

For laminar flow, the viscous effects, and therefore the inner region, extend through the whole profile. It is universally accepted that for laminar wedge flow, the Falkner-Skan [20] equations are solutions to the flow governing equations. For this case, the similarity length scaling parameter is proportional to

$$\delta(x) = \sqrt{\frac{2}{m+1} \frac{\nu x}{u_e}} \quad (23)$$

where m is a constant dependent on the wedge angle and the similarity velocity scaling parameter is u_e is given by

$$u_e = kx^m. \quad (24)$$

The velocity at the boundary layer edge u_e is the similarity velocity scale. If the Prandtl velocity scale u_τ is also a similarity velocity scale, then the velocity ratio

$$e(x) = \frac{u_e}{u_\tau} \quad (25)$$

must be equal to a non-zero constant. The friction velocity is defined by Eq. 8 and the derivative at the wall can be written as

$$\left\{ \frac{\partial u}{\partial y} \right\}_{y=0} = \frac{u_e}{\delta(x)} \left\{ \frac{\partial u/u_e}{\partial y/\delta(x)} \right\}_{y=0}. \quad (26)$$

By the definition of similar profiles the quantity in the braces on the right-hand-side of Eq. 26 must be a constant that we will designate as l . Therefore, combining Eqs. 8, 25, and 26, we have

$$e(x) = \frac{u_e}{u_\tau} = \frac{u_e}{\sqrt{l \frac{u_e}{\delta(x)}}}. \quad (27)$$

Substituting in Eqs. 23 and 24, it is obvious that $e(x)$ is, in general, not a non-zero numerical constant (except for sink flow, $m = -1$) for laminar flows. Therefore the Prandtl velocity scale is not a similarity constant for 2-D laminar wedge flow. Using a similar development, it is also

possible to show that the Prandtl length scale ν/u_τ is not a similarity scaling variable for 2-D laminar flow over a wedge.

Contrast this with the μ_1 scaling parameter. In the last Section, we showed that the scaling variable μ_1 and u_e must be a similarity scaling parameters for all 2-D wall bounded similarity flows. For verification purposes, it easy to show that for similarity of laminar wedge flow discussed in this Section, that the ratio given by

$$g(x) = \frac{\delta(x)}{\mu_1} \quad (28)$$

is equal a non-zero numerical constant. Using Eqs. 2 and 26, and the fact that the quantity in the braces on the right-hand-side of Eq. 26 must be a constant, then it easy to show that in fact $g(x) = l$. Therefore, the new length scale μ_1 and velocity scale u_e are similarity scaling parameters for 2-D laminar flow over a wedge in agreement with the results of the last section.

4.2 Inner Region Turbulent Flow Similarity

For inner layer similarity scaling of the turbulent boundary layer, decades of experimental work have convinced most researchers that the Prandtl scaling is the correct scaling for the inner region. The reason now becomes clear given that the Prandtl length scale is actually the mean location of the second derivative of the velocity profile. The second derivative of the velocity is directly responsible for the viscous forces acting in the near wall region of the boundary layer and the viscous forces are one of the major forces controlling the fluid flow in the near wall region. The mean location of the second derivative of the velocity relative to the wall is therefore tracking the major flow controlling force in the near-wall region. For the turbulent boundary layer, Prandtl showed that the region just above the viscous sub-layer, the Log law region, is also controlled by the wall shear stress.

While the moment description makes it clear why the Prandtl scaling works, the question becomes how does the new scaling μ_1 compare with the Prandtl scaling. This parameter should also be tracking the viscous forces. In Figs. 3-5 we compare the Prandtl scaling and the μ_1 scaling for the inner region of three different experimental turbulent boundary layer datasets. In these plots the same number of data points are used in each comparative plot, *e.g.* Fig. 3a and 3b. The upper range of the x -axis was chosen to roughly correspond to the upper range of the viscous region ($\sim 2\mu_1 = \sim 60-110\nu/u_\tau$). For Figs. 3 and 4, we observe that the Prandtl scaling does indeed result in better velocity profile similarity over the viscous region.

How then does one explain the plots in Fig. 5? Why is this dataset showing reasonable similarity even for the μ_1 -scaled profiles? The answer is tied to the u_e/u_τ ratio, the Rotta condition. If the Rotta condition holds (Eq. 22), then the new scaling and the Pradtl scaling become identical. The datasets illustrated in Figs. 3-5 were selected to show the effect of the Rotta condition. To quantify how close we are to satisfying the Rotta condition we calculated the maximum percentage difference from the average u_e/u_τ value for each set of velocity profiles. For the DeGraaff and Eaton dataset (Fig. 3) this difference is $\pm 8\%$, for the Österlund dataset (Fig. 4) it is $\pm 4\%$, and for the Skåre and Krogstad dataset (Fig. 5) it is $\pm 2\%$. It is obvious that the closer the data comes to satisfying the Rotta condition, the more the μ_1 -scaled

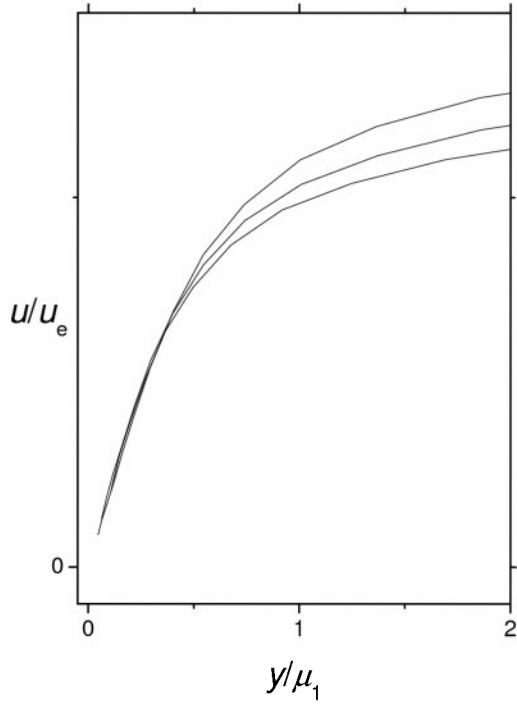


Figure 3a: DeGraaff and Eaton [5] velocity profiles taken at $Re_\theta=1430$, 2900, and 5200.

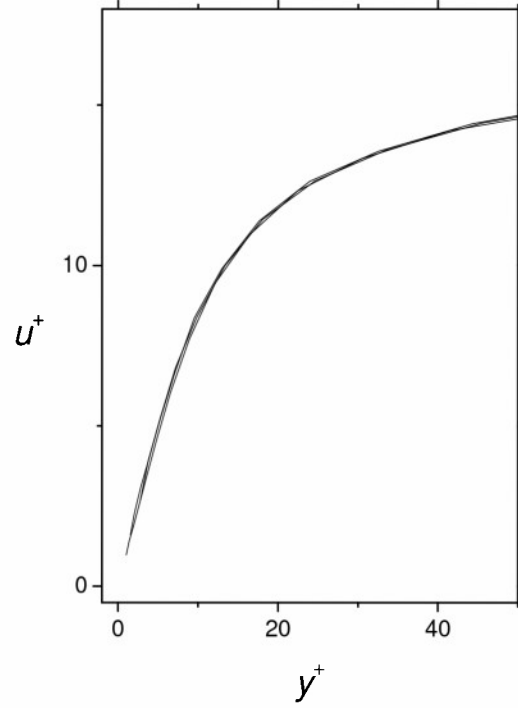


Figure 3b: DeGraaff and Eaton [5] velocity profiles taken at $Re_\theta=1430$, 2900, and 5200.

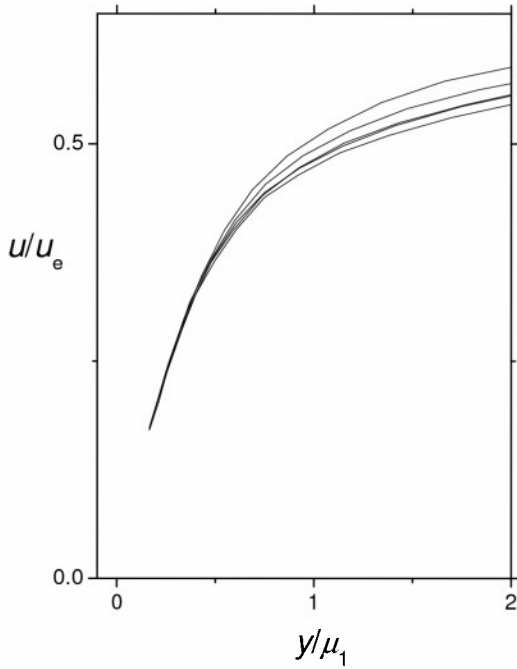


Figure 4a: Five Österlund [21] velocity profiles for $u_e \approx 10.3$ m/s.

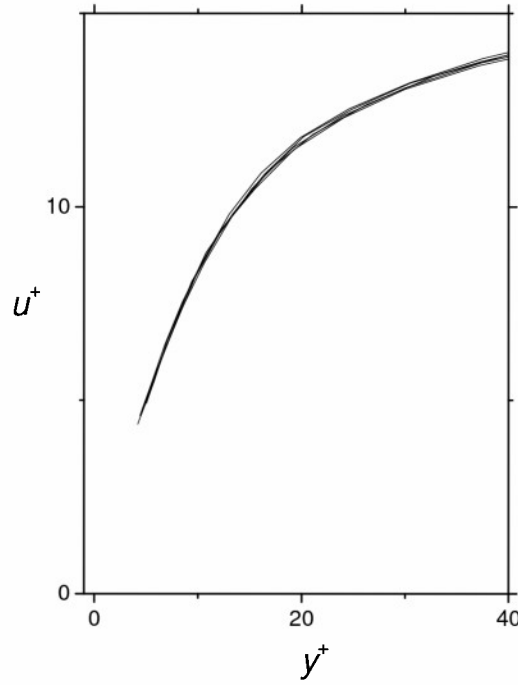


Figure 4b: Five Österlund [21] velocity profiles for $u_e \approx 10.3$ m/s.

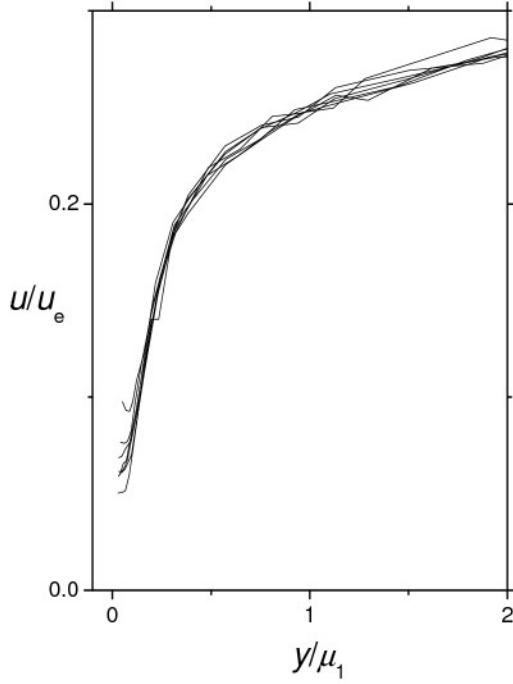


Figure 5a: Skåre and Krogstad [22] seven velocity profiles.

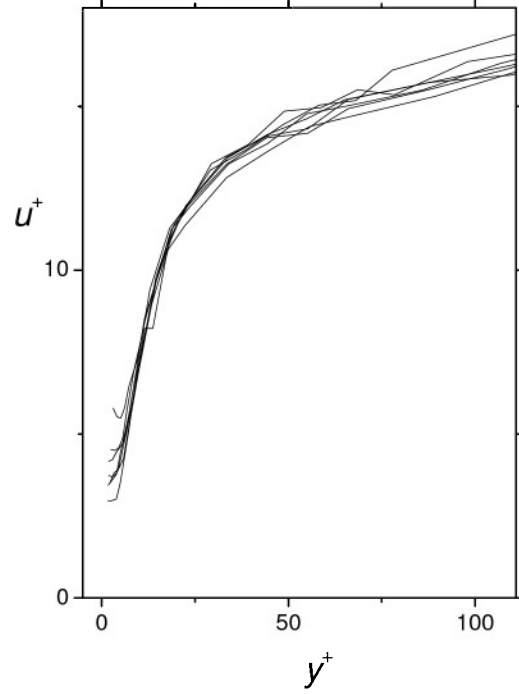


Figure 5b: Skåre and Krogstad [22] seven velocity profiles.

plots display similarity-like behavior through the whole viscous region of the turbulent boundary layer. This confirms our expectations that the Prandtl scaling and the new scaling μ_1 and u_e should be equivalent if the Rotta condition is satisfied.

4.3 Whole Profile Turbulent Flow Similarity

The results displayed in Fig. 5 are intriguing. Although we are interested in inner layer scaling herein, it is notable that according to Section 3 above, μ_1 and u_e could also be scaling variables that result in similarity over the whole profile, not just the inner region. If one examines Fig. 5a and 5b, the plots appear similar within experimental error. To test to see if the new scaling extends to the whole profile similarity we expand the view of Fig. 5a and 5b to show the whole profile in Fig. 6a and 6b. Obviously, these figures indicate that neither μ_1 and u_e nor the Prandtl scaling result in whole profile similarity. However, Weyburne [16] showed that to experimental accuracy, certain turbulent boundary layer flow datasets do display whole profile similarity, including the Skåre and Krogstad [22] dataset, if they are scaled using δ_1 and u_e . This scaling is illustrated in Fig. 7. This figure exhibits excellent collapse of all seven profiles to a single curve. If whole profile similarity exists in a set of profiles, then δ_1 and μ_1 should both

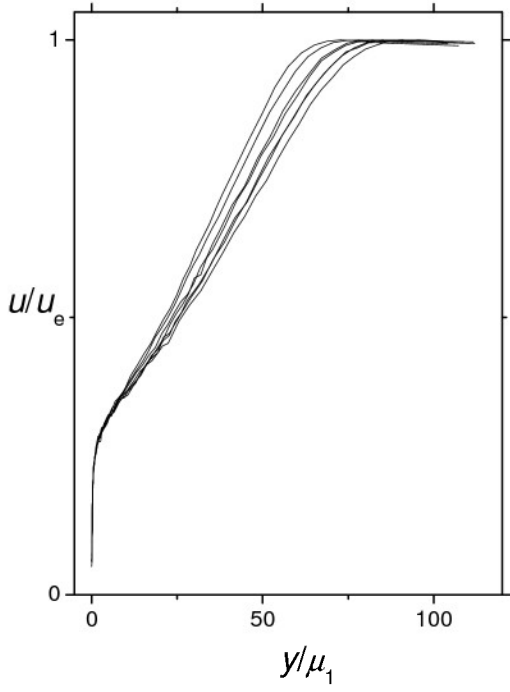


Figure 6a: The rescaled velocity profiles from Skåre and Krogstad [22].

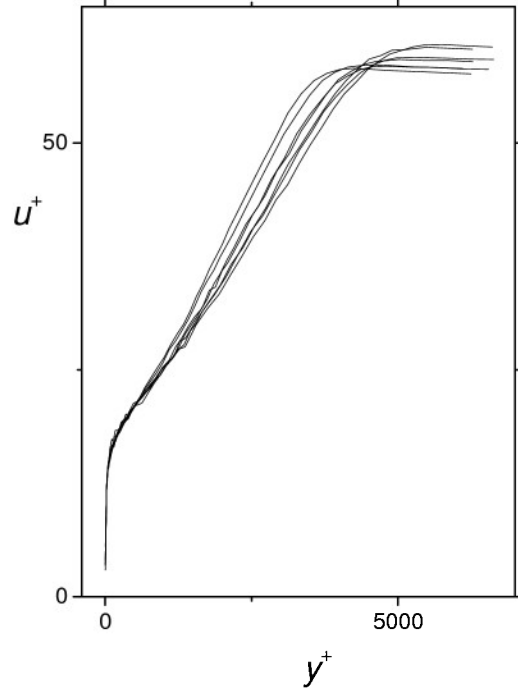


Figure 6b: The rescaled velocity profiles from Skåre and Krogstad [22].

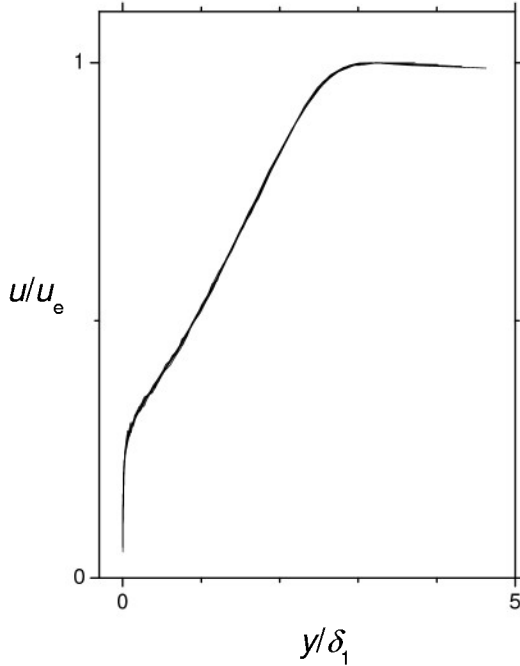


Figure 7: The seven velocity profiles from Skåre and Krogstad [22].

be similarity scaling variables according to Eq. 19.

How can this apparent contradiction be explained? One possibility is that the c_f data, which is used to calculate μ_1 and u_τ , is in error. Consider that Skåre and Krogstad used three indirect methods for obtaining c_f (from which μ_1 and u_τ are calculated). In Fig. 8, we reproduce Skåre and Krogstad Fig. 4a plot of their c_f data. The open circles were obtained by Skåre and Krogstad using a fitting technique involving the Musker semi-analytical velocity profile and apparently are the values tabulated in Skåre and Krogstad's Table 1. The diamonds are from Preston tube measurements and the open circles were obtained by a shear stress balance equation approach. Notice that there is up to a 10% variation between the fitted method and Preston tube method and up to a 30% variation between the fitted method and shear

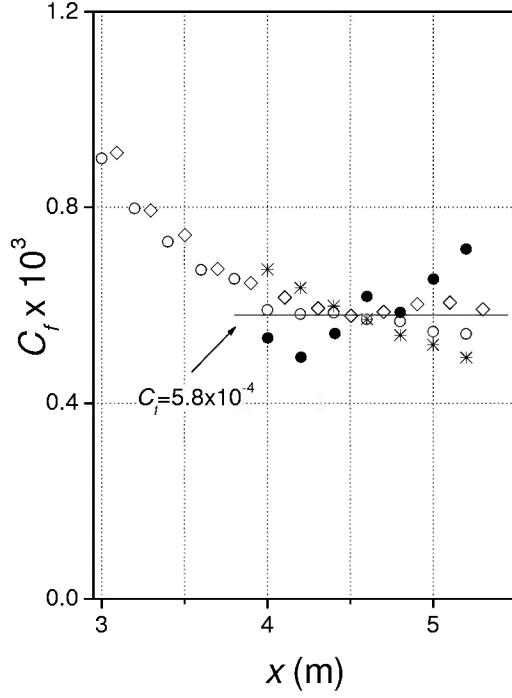


Figure 8: A reproduction of Skåre and Krogstad's [22] Fig. 4a showing their reported c_f data

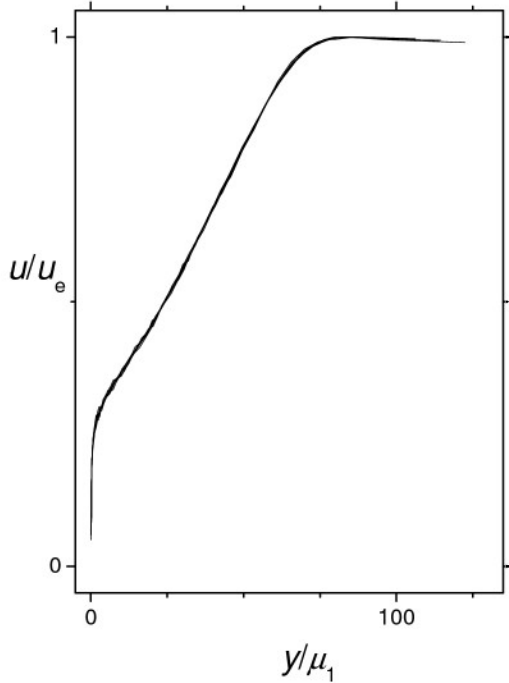


Figure 9: Seven velocity profiles from Skåre and Krogstad [22] using inferred μ_1 values.

stress method. Furthermore, the tabulated values found in the paper are based on a velocity profile fitting method that utilizes the Musker approximate profile for the inner region. It is known, however, that the Musker profile is only applicable to the ZPG turbulent profiles, not the adverse pressure gradient (APG) profiles of Skåre and Krogstad. Therefore it is not unreasonable to expect that values reported by Skåre and Krogstad are possibly in error by a small percentage.

We therefore set out to find an “inferred” c_f dataset. To obtain an inferred c_f dataset, we note that according to Eq. 15, the ratio of δ_1 to μ_1 should be a constant for similarity. Using the tabulated c_f data to calculate μ_1 , the variation of the ratio δ_1/μ_1 is from +11% to -11% from the average. We therefore calculated an inferred μ_1 data set that had the same average value as Skåre and Krogstad's fitted data, but with μ_1 having the same linear variation as their δ_1 data. This data is used to calculate an inferred c_f dataset that is depicted by stars in Fig. 8. The difference between the inferred c_f and the tabulated c_f data is on the order of $\pm 10\%$. If one uses this inferred μ_1 data, then one obtains the plot shown in Fig. 9. Obviously the inferred μ_1 data results in similarity-like behavior.

The inferred scaling results are at least plausible. To strengthen the case we looked at the other two turbulent datasets that also showed whole profile similarity using δ_1 and u_e scaling [14]. The datasets include the last five profiles of Clauser's [23,24] first dataset and the last four profiles of Herring and Norbury [24,25] first dataset. For the Clauser dataset, the variation of the inferred c_f values differ from the reported values is +11% to -26%. For the Herring and Norbury dataset, the variation of the inferred c_f values differ from the reported

values from $\pm 10\%$. Rather than essentially reproducing the plots from Weyburne [14] (with μ_1 instead of δ_1), we merely note that the plots using the inferred μ_1 do indeed produce the appearance of whole profile similarity.

It is important to point out that in all three datasets, the inferred c_f data shows linearly decreasing behavior as one moves further out on the wedge as shown for example in Fig. 8. However, if the Rotta condition holds, *i.e.* $u_e/u_\tau = \text{constant}$, then the c_f data should be a constant. This problematic behavior will be discussed in the Discussion section below.

5. Conceptualizing the Turbulent Boundary Layer

What emerges from this work together with an earlier study on outer region similarity [16] by this author is a different conceptual picture from that which has been built up since Prandtl's [3] pioneering work. In order to understand the differences, we begin by first reviewing the current conceptual picture of the turbulent boundary layer. Buschmann and Gad-el-Hak [26] have presented an excellent review of the present state of scaling of the turbulent boundary layer. In what follows we give a very condensed version of the present state of our understanding of scaling for the turbulent boundary layer.

5.1 Current Scaling Model

In the early Prandtl model of the turbulent boundary layer, although the Log Law applied to the overlap region it was assumed that this single length and velocity scale characterizes the entire boundary layer. It was soon realized that the Prandtl length and velocity scale did not work over the whole profile. This led to the concept of an inner and outer layer. This has evolved to where it is now assumed the regions are essentially separate and that one could have one set of similarity scaling parameters in the inner region and possibly a separate set of scaling parameters applying to the outer region (see for example discussion in Coles and E. Hirst [24]). The Log Law, or the competing laws detailed in Buschmann and Gad-el-Hak [26] review, generally apply to the overlap region between the inner and outer region. In all of the competing theories, the Prandtl scaling parameters are used. Although never explicitly tested, experimental evidence seems to indicate that the Prandtl scaling also applies to the inner near-wall region. Thus the current model has the inner layer length scaling as ν/u_τ and the inner layer velocity scaling as u_τ . Furthermore, this scaling applies to most if not all turbulent boundary flows.

For the outer region, Brezek, *et. al.* [27] presents a good historical summary of scaling of the outer region. The modern search for similarity scaling behavior for the outer layer began with the experimental and theoretical work of Clauser [23]. Using the friction velocity u_τ as the velocity scaling variable for the outer region, Clauser predicted that equilibrium (similar) boundary layers are only obtained for the nonzero pressure gradient case when

$$\beta_\tau = -\frac{\delta_1}{\rho u_\tau^2} \frac{dp_e}{dx} \quad (29)$$

is a constant. Based on Eq. 29 criteria, Clauser was able to generate similarity-like behavior for certain turbulent flows and found that, in general, the experimental equilibrium similarity condition is relatively rare and difficult to generate.

Rotta [15] and Townsend [28] subsequently developed some additional theoretical conditions for turbulent boundary layer similarity. Like Clauser, Rotta made specific assumptions about the velocity scaling ($=u_\tau$) and the Reynolds stress scaling ($=u_\tau^2$). More recently, Castillo and George [29] used a momentum balance approach and found that the free stream velocity u_e must be the velocity scaling parameter of flows with a pressure gradient. In addition, they found that similarity exists only when the parameter defined as

$$\Lambda \equiv -\frac{\delta du_e/dx}{u_e d\delta/dx} = \text{constant} \quad (30)$$

where δ is the thickness scaling parameter. Taking δ equal to the ninety-nine percent thickness δ_{99} , Castillo and George showed that rather than being rare, most nonzero pressure gradient turbulent boundary layer flows with constant upstream conditions were in equilibrium by this measure. In fact, they showed that only three values of this pressure parameter were needed to characterize all equilibrium turbulent boundary layers. One was for the APG flow with $\Lambda = 0.22$, one for the favorable pressure gradient (FPG) flow with $\Lambda = -1.92$, and one for the ZPG flow with $\Lambda = 0$. In one of the most recent publication by Castillo and co-workers, Cal and Castillo [30] backed off from this strong stance indicating other values for Λ are possible. Nevertheless, they indicate that even for the nonequilibrium flow cases ($\Lambda \neq \text{constant}$), most flows show good collapse of the defect profile $(u_e - u(x, y))/u_s$ when the length scaling parameter is δ_{99} or δ_{95} and the velocity scaling parameter u_s is the Zagarola and Smit velocity scale $u_{zs} = \delta_1 u_e(x)/\delta_{99}$ rather than u_e as originally advocated by Castillo and George. Therefore, for the outer region, the current model for scaling is that the length scaling parameter is δ_{99} or δ_{95} and the velocity scaling parameter is u_{zs} . Furthermore, most turbulent boundary layers show good collapse of the defect profile $(u_e - u(x, y))/u_{zs}$ when using this scaling combination.

5.2 New Scaling Model

In the new model, the inner layer designation will be replaced with the Prandtl layer designation. Although the extent and scaling are identical, we will use the Prandtl layer designation to emphasize the differences. For the Prandtl layer, the length still scales as ν/u_τ and the velocity scales as u_τ . Furthermore, this scaling applies to most if not all turbulent boundary flows. What is different is the realization that the Prandtl scaling works because the Prandtl mean location ν/u_τ parameter tracks the viscous flow contributions for the turbulent flow case. It also becomes apparent why the Log Law has been so successful. If one examines Fig. 2, then one sees that the curve to the right of the peak is not falling exponentially to zero as is the case for a Gaussian-like curve (Fig. 1). Instead, the second derivative curve is slowly decaying to zero in a $\sim 1/y^2$ fashion. This leads to a logarithmic velocity profile in the region just above the peak in the viscous region. Thus the Log Law is simply the result of the fact that the viscous forces, which are being tracked by the Prandtl scaling parameters, is decaying to zero in a $\sim 1/y^2$ fashion instead of exponentially (more about this in the Discussion below). This means that the viscous forces are controlling the Log Law region in the turbulent boundary layer.

These simple observations make it obvious as to why the Prandtl scaling have been so successful.

In the very near wall region ($0 < y/\mu_1 < 0.2$ which corresponds to $0 < y^+ < 5$), the current model assumes that the velocity profile is a linear function of the distance. This is incorrect as is evidenced by Figs. 1 and 2. The second derivative of a linear function is zero and as is obvious from Figs. 1 and 2, there is no place in this region where the second derivative is zero (except at $y=0$). The problem with continuing to assume linear behavior is that this would mean there would be no viscosity contribution to the flow in this region. In fact the opposite is true; the viscosity contribution basically peaks at $y/\mu_1 \sim 0.2$ ($y^+ \sim 5$). The behavior is better described as being linear-like with a quartic component in this region [9].

For the outer region, we note that the Castillo, George, and coworkers model is still being adjusted as new results are introduced. However, there have been some indications that this model for the turbulent boundary layer may not represent the correct picture. Indeed, Maciel, Rossignol, and Lemay [31] considered the Castillo and George formulation and, after looking at a range of experimental datasets, concluded that universal similar profiles for the ZPG, APG, and FPG boundary layers do not exist. While they concede the existence of similarity-like behavior in certain sets of experimental profiles, they contend that most turbulent boundary layers found in the real world are almost never in a state of equilibrium as contended by Castillo and George.

More recently, Weyburne [16] showed that the supposed success of the Castillo and George model is being realized because of a flaw in the way the plots are being presented. The problem is that similarity behavior is being claimed by plotting datasets using the defect profile $(u_e - u(x, y))/u_{ZS}$ plotted versus y/δ_{99} . We have found that the defect profile tends to hide scaling differences in the outer region. Weyburne [16] showed that if one replots the data used by Castillo and George using the y -axis scale u/u_{ZS} instead of $(u_e - u)/u_{ZS}$, then the profiles do not show good collapse as contended by Castillo and George. Because of the importance of this point, we offer additional support for this lack of similarity behavior. According to Cal and Castillo [30] even nonequilibrium flow cases ($\Lambda \neq \text{constant}$) should show good collapse of the defect profile $(u_e - u(x, y))/u_{ZS}$. In Fig. 10a we reproduce part of Cal and Castillo [30] Fig. 2b. This figure shows data from Schubauer and Klebanoff [32] consisting of ten nonequilibrium profiles (taken at the 21 ft to the 25.77 ft stations). The profiles shown in Fig. 10a collapse reasonably well. Now consider the same exact data plotted in Fig. 10b using the y -axis scale u/u_{ZS} instead of $(u_e - u)/u_{ZS}$. Recall the definition of similarity is that two velocity profiles are similar if they differ only by a scaling constant in y and $u(x, y)$ for all y -values. Obviously, the ten profiles in Fig. 10b do not show similarity. This result, along with the earlier work [16], makes us believe that Castillo and George's [29] contention that most turbulent boundary layers are in equilibrium is in error.

What emerges from the results herein and the earlier work is a very different picture of the outer turbulent boundary layer. In fact, we reject the traditional two-layer model. Instead, we believe that what we have is an inner layer similarity wall region in which the length and velocity scaling is controlled by the viscosity. Rather than an outer region with a distinct set of scaling, in the new model what we have is that for a small subset of turbulent boundary layers, whole profile similarity begins to turn on under the right conditions. Thus the previous work on outer layer similarity was actually discovering whole profile similarity-like behavior rather than

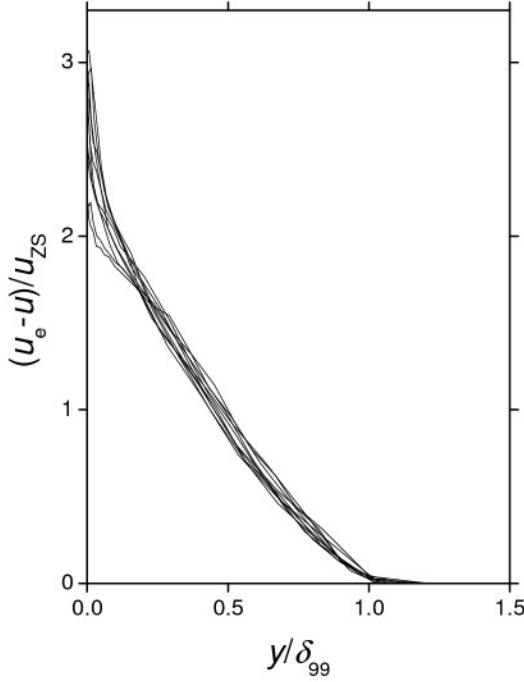


Fig. 10a: Ten profiles from Schubauer and Klebanoff [32].

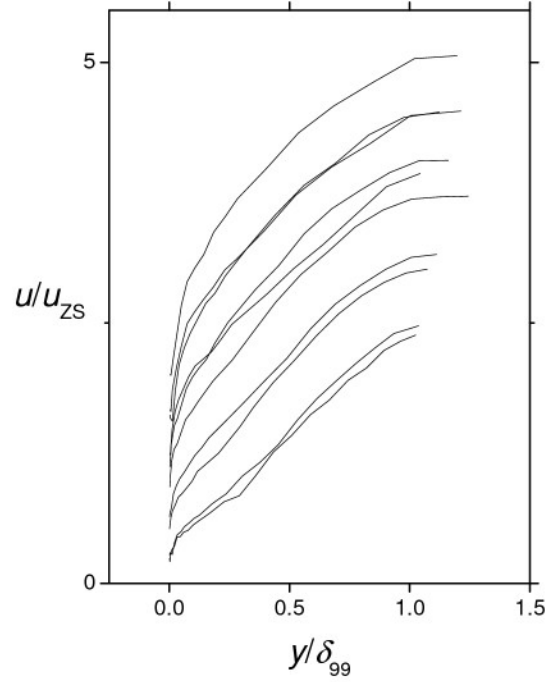


Fig. 10b: Ten profiles from Schubauer and Klebanoff [32].

outer layer similarity that is somehow distinct from the inner layer similarity. Note that according to the old conceptual model, whole profile similarity is not even possible for turbulent boundary layer flows. This point will be discussed more fully in Section 6 below. Suffice it to say that the argument for whole profile similarity of the turbulent boundary layer is very compelling.

The conditions for whole profile similarity follow from the momentum balance approaches presented by previous authors [23, 28, 29, 31, and 16]. They consist of: 1) the thickness scales as a linear function of the distance along the plate, 2) the velocity scales as the free stream velocity u_e and is a power function of the type $u_e = a_1(x - x_0)^m$, 3) the Reynolds stress scales as $uv(x) = u_\tau^2$ and $uu(x) = u_\tau^2$ or $uu(x) = u_e u_\tau$ [16]. However, the primary condition for whole profile similarity is the Rotta condition holds; that is the ratio u_e/u_τ is (almost) constant. Traditionally, one views this ratio as the equivalence of the inner to outer velocity scales. In addition, under this condition, the length scales δ_1 , μ_1 , and ν/u_τ become equivalent. If the conditions 1-3 holds along with the Rotta condition, then the Clauser pressure condition (Eq. 28) becomes equivalent to Castillo and George's pressure condition (Eq. 27) and both are satisfied.

Experimentally, the Rotta condition appears to be difficult to achieve. For datasets where the ratio difference is on the order of 10% or less, the velocity profiles start to show similarity-like behavior. This similarity-like behavior first manifests itself as what has been traditionally called the outer region similarity. Thus, all previous claims of outer region similarity are actually the beginning of whole profile similarity. However, it is not until the ratio difference becomes on the order of 2% or less that the profiles start to show whole similar to experimental accuracy.

6. Discussion

In this paper we reviewed a second derivative moment method that can track the viscous region of any 2-D wall bounded flow, including laminar, transitional, and turbulent boundary layer flows. The big advantage of the moment method is that the handful of moment-based parameters can be traced back to the physical structure of the boundary layer. In particular, the μ_1 parameter is the mean location of the second derivative profile for laminar flow and the Prandtl length scale ν/u_τ is the mean location of the second derivative profile for turbulent flow. It should also be noted that the displacement thickness δ_1 is mean location of the first derivative of the velocity profile, which means it tracks the outer region of the velocity profile [13]. This explains why Weyburne [14] found that δ_1 was effective as a similarity parameter for the outer region of certain turbulent boundary layers. Note however, that according to the new conceptual model, it was not outer region similarity that was being discovered using the Rotta condition as a screening tool in the Weyburne [14] paper, rather it was the beginning of whole profile similarity-like behavior. The parameters μ_1 and δ_1 are just two of the moment-based parameters that can be used to describe the boundary layer thickness and shape [12,13].

The moment method was instrumental in showing that the reason for the success of the Prandtl scaling is that the Prandtl length scale ν/u_τ is actually the mean location of the second derivative profile for the turbulent boundary layer. This means that ν/u_τ tracks the viscous contributions for the turbulent flow case. The viscous contributions in turn control the flow behavior in the near wall region. We note that the development of the wall based moments in Section 2.2 required that we take the integral limit using wall-based friction velocity units rather than in the free stream velocity units. The justification for this is mostly experimental as is evidenced by Figs. 3-5. The wall-based Prandtl scaling units result in near wall similarity whereas the free stream scaling units μ_1 do not. Furthermore, taking the integral limit out to the free stream located at about $y \cong 1070\nu/u_\tau$ compared to the near wall value at $y \cong 70\nu/u_\tau$ makes only an insignificant change (less than 1%) in the value of the mean location calculated using Eq. 10. What it does do is significantly change the x -dependence of the mean location value. We therefore feel justified in the wall moment development leading to the connection of the Prandtl length scale and the mean location of the second derivative profile.

Not only does the second derivative wall moment development explain the success of the Prandtl scaling in the viscous region, but it also makes it apparent why the Log Law has been so successful. If one examines Fig. 2, then one sees that the curve to the right of the peak is not falling exponentially to zero as is the case for a Gaussian-like curve (Fig. 1). Instead, the second derivative curve is slowly decaying to zero in a $\sim 1/y^2$ fashion. To emphasize this point, we replot Fig. 2 using log Plus units in Fig. 11. In this plot, the DNS data (+) shows Log Law behavior (the red line is the second derivative of Eq. 1) starting in the region just about at the peak in the viscous region. We should point out that this $\sim 1/y^2$ decay is the result of the time averaging of the profiles. It may be that if one were able to look at the instantaneous velocity profiles, the instantaneous second derivative profile may still fall to zero exponentially but, as a result of the spatial averaging due to the time averaging process, the time averaged curve appear to be decaying in a $\sim 1/y^2$ fashion. Even though the viscous forces are fairly small in the Log

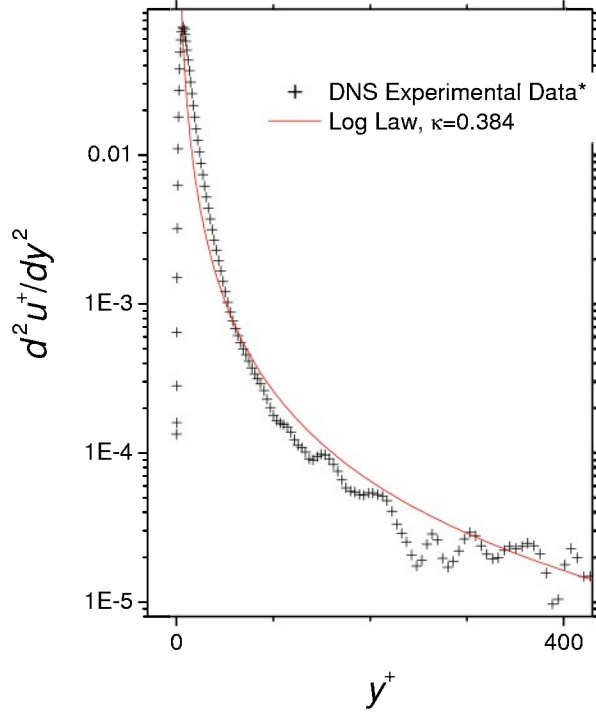


Figure 11: The DNS solution for the ZPG turbulent boundary layer from Khujadze and Oberlack [19].

Law region compared to the peak value, it is apparent that they are still controlling the flow behavior in this region. This observation is supported by the work of Sreenivasan and Sahay [33] who pointed out that the Reynolds shear stress contribution to the momentum balance in the Log Law region must go to zero. This indicates that the viscous effects must play an important role in the region traditionally thought to be inviscid. Hence, not only does the Log Law region extend much further toward the wall than traditionally thought, but the viscous forces have important contributions throughout the entire Log Law region. Since the Prandtl length scale is the mean location of the viscous forces, then it becomes clear as to why the Prandtl scaling have been so successful.

The equal area integral approach to investigating similarity and the traditional momentum balance approach are actually complimentary approaches. The integral approach is effective at identifying which scaling parameters are actually similarity

parameters. For example, for the 2-D boundary layer flow case, we proved theoretically that if whole profile similarity exists in a set of velocity profiles taken at various points along the flow direction, then the μ_1 and δ_1 must be a similarity length scaling parameters. The associated velocity scaling parameter is u_e . For the case where the Rotta condition holds (Eq. 22) identically, we showed that in fact δ_1 , Δ , μ_1 , and ν/u_τ all must be similarity length scaling parameters and u_e , u_τ , and u_{zs} (the Zagarola and Smit velocity scale) must be similarity velocity scaling parameters (Δ is the Clauser-Rotta lengthscale, $\delta_1 u_e / u_\tau$). The momentum balance approach on the other hand is effective at identifying the properties that scaling parameters must have for similarity to exist. We note that there is one exception to this general division of the two similarity approaches. Castillo and George [29] used the momentum balance approach to show that for turbulent flows with a pressure gradient, the velocity scaling parameter for similar flows must be u_e in agreement with the integral approach.

Conventional thinking is that this whole profile similarity scenario is not possible for turbulent boundary layers. The conventional wisdom case is based on the argument that the x -dependent variable groupings appearing in the flow momentum equations must have the same functional dependence as the flow develops along the plate (wedge). Townsend [28] used this approach to show that if one includes the viscous force term parameter for turbulent flows, then these parameter ratios require that the thickness scaling must be linear in x and that the velocity

scaling must go as $1/x$ (*i.e.*, wedge sink flow). These results are indisputable. However, as Weyburne [14] pointed out, the momentum equation argument does not account for the magnitude of the viscosity term as one proceeds down the wedge, or in this case the variation of the magnitude of the term as one proceeds down the wedge. Since the flow governing equations are partial differential equations, it is always necessary to neglect certain terms because their magnitude is small relative to the other terms in order to obtain similarity solutions. It is our contention that for certain turbulent boundary layer flows, that while the magnitude of the viscous term in the momentum equation is not negligible as one proceeds down the length of the wedge, the variation of the magnitude of the term is smaller than what can be measured experimentally. Weyburne [14] presented semi-empirical based arguments that indicate that the viscous term variation as one proceeds down the length of a wedge for certain turbulent flows is indeed small. Therefore, even if the Townsend based requirements are violated, it is still possible to have whole profile similarity within experimental error for certain 2-D wall bounded turbulent boundary layer flows. Weyburne [14] presented the experimental data of Clauser [23], Herring and Norbury [25], and Skåre and Krogstad [22] as showing whole profile similarity. Results presented herein using the same datasets with the inferred c_f data are not definitive but they are plausible and therefore tend to support the proposition that whole profile similarity is possible for the turbulent boundary layer.

The strongest support for the violation of the Townsend viscosity-based similarity argument for the turbulent boundary layer comes from the near universality of the Prandtl scaling applying to the inner region. Although we have presented a moment-based theoretical foundation for this universality of the Prandtl scaling, it has never been experimentally tested specifically for applicability in the inner region to our knowledge. However, there are many papers that have considered the universality of the Log Law region (see for example Monkewitz, Chauhan, and Nagib [4]). Although the Log Law region does not extend to the wall, there have been a few experimental papers [5-6] as well as a few papers [7-9] that use analytical extensions to the Log Law that cover the region from the wall out to the outer limits of the Log Law region. These papers indicate that even in the inner viscosity dominated region, the Prandtl scaling produces similar-like velocity profiles all the way to wall. Consider, for example, Figs. 3b, 4b, and 5b that show good collapse of the sets of velocity profiles well into the viscous region. How is this possible in light of the Townsend based viscosity argument? According to Townsend's viscosity argument, inner layer similarity should not be possible for the turbulent boundary layer except for sink flow. The only answer that makes sense is that, as we have already contended above; the expected differences in the velocity profiles due to viscosity must be smaller than what can be measured experimentally.

Additional support for the whole profile similarity scenario comes from an earlier paper by Weyburne [16] who investigated outer region similarity of the turbulent boundary layer. In this paper, it was pointed out that the only datasets showing outer region similarity were datasets that satisfied the Rotta condition. Using the Rotta condition as a screening tool, eleven datasets from various authors were found that satisfy the Rotta condition approximately, including the Skåre and Krogstad [22] dataset. In that study, four possible length scales (δ_1 , Δ , δ_2 , and δ_{99}) and three possible velocity scales (u_e , u_τ and u_{ZS}) were compared [16]. By comparing plots, it was found that all of the length scales produced similar results. However, in general, δ_1 and u_e resulted in the best similarity-like scaling. In retrospect, it may be that δ_1 and u_e have the

smallest measurement error bars. On the other-hand, u_τ measurements are all indirect and have the most uncertainty. In any case, the fact that a purely experimental comparison found that δ_1 and u_e resulted in the best similarity-like scaling in outer region of the turbulent boundary layer cannot be a mere coincidence. Instead, it supports the contention that whole profile similarity is possible for the turbulent boundary layer and is consistent with the new conceptual picture of the turbulent boundary layer developed in Section 5.

Strictly speaking, whole profile similarity is only possible for $u_e/u_\tau = \text{constant}$. Experimentally, it would seem that it is not possible to achieve this goal exactly. Rather one can come close, as with the Skåre and Krogstad [15] dataset. Consider the c_f data shown in Fig. 8. If $u_e/u_\tau = \text{constant}$ condition holds, then c_f must be a constant. Yet the inferred dataset (stars), which produces similarity-like behavior of the velocity profiles, is not constant and is in fact a linearly decreasing function of the plate Reynolds number. We believe that this behavior is a reflection of the fact that the viscous forces are working against perfect velocity profile similarity. It just happens that the differences in the profiles are smaller than the experimental uncertainty as long as the u_e/u_τ ratio spread is on the order of $\pm 2\%$ or less (corresponding to a skin friction coefficient spread of about $\pm 10\%$).

7. Conclusion

Using the moment method that was previously used to develop length scaling parameters for describing the boundary layer region, it was discovered that the Prandtl length scale is actually the mean location of the second derivative of the velocity profile for the turbulent boundary layer. This discovery makes it clear as to why the Prandtl scaling has been so successful. In addition, it was shown that for whole profile similarity of 2-D wall bounded velocity profiles, the second derivative based thickness parameter μ_1 must be a similarity length scaling variable and the velocity scaling variable must be the free stream velocity. It was shown that to experimental accuracy, this parameter may show whole profile similarity for certain turbulent boundary layer datasets satisfying the Rotta condition. Finally, a new conceptual picture of the turbulent boundary layer was presented. It is better able to explain the nature of the turbulent boundary layer than the current model.

8. References

- [1] Reynolds, O., “An experimental investigation of the circumstances which determine whether the motion of water in parallel channels shall be direct or sinuous, and of the law of resistance in parallel channels,” *Philosophical Transactions of the Royal Society of London*, vol. 174, 935(1883).
- [2] Prandtl, L., “Zur Turbulenten Strömung in Rohren und längs Platten.”, *Ergeb. Aerod. Versuch Göttingen*, TR 4, 1932.
- [3] George, W., “Recent Advancements Toward the Understanding of Turbulent Boundary Layers.” *AIAA Journal*, Vol. 44, 2435(2006).
- [4] Monkewitz, P., Chauhan, K., and Nagib, H., “Comparison of mean flow similarity laws in zero pressure gradient turbulent boundary layers,” *Phys. of Fluids*, vol. 20, 105102(2008).
- [5] DeGraaff, D. and Eaton, J., “Reynolds number scaling of the flat plate turbulent boundary layer,” *J. Fluid Mech.*, vol. 422, 319(2000).
- [6] Poggi, D., Porporato, A., and Ridolfi, L., “An experimental contribution to near-wall measurements by means of a special laser Doppler anemometry technique”, *Experiments in Fluids*, vol. 32, 366(2002).
- [7] Monkewitz, P., Chauhan, K., and Nagib, H., “Self-consistent high-Reynolds-number asymptotics for zero-pressure-gradient turbulent boundary layers,” *Phys. of Fluids*, vol. 19, 115101(2007).
- [8] Kendall, A., and Koochesfahani, M., “A method for estimating wall friction in turbulent wall-bounded flows,” *Exp Fluids*, vol. 44, 773(2008).
- [9] Weyburne, D., “A Velocity Profile Approximation for the Inner Region of the Turbulent Boundary Layer in an Adverse Pressure Gradient”, *US Air Force Technical Report AFRL-RY-HS-TR-2010-0015*, 2010.
- [10] Buschmann, M. and Gad-el-Hak, M., “Structure of Turbulent Boundary Layers with Zero Pressure Gradient,” *AIAA paper Number 2005-4813*, 2005.
- [11] Zagarola, M. and Smits, A., “Mean-flow scaling of turbulent pipe flow,” *J. Fluid Mech.*, vol. 373, 33(1998).
- [12] Weyburne, D., “A mathematical description of the fluid boundary layer,” *Applied Mathematics and Computation*, vol. 175, 1675(2006). Also Weyburne, D., “Erratum to “A mathematical description of the fluid boundary layer” ,” *Applied Mathematics and Computation*, vol. 197, 466(2008).

- [13] Weyburne, D., “New Shape Parameters for the Laminar, Transitional, and Turbulent Velocity Profiles”, US Air Force Technical Report AFRL-RY-HS-TR-2010-0016, 2010.
- [14] Weyburne, D., “The Mathematics of Flow Similarity of the Velocity Boundary Layer”, US Air Force Technical Report AFRL-RY-HS-TR-2010-0014, 2010.
- [15] Rotta, J., “Turbulent Boundary Layers in Incompressible Flow,” Prog. Aerospace Sci., vol. 2, 1(1962).
- [16] Weyburne, D., “Similarity of the Outer Region of the Turbulent Boundary Layer,” US Air Force Technical Report AFRL-RY-HS-TR-2010-0013, 2010.
- [17] Blasius, H., Z. Math. Phys., “Grenzschichten in Flüssigkeiten mit kleiner Reibung,” vol. 56, 1(1908).
- [18] Schlichting, H., *Boundary Layer Theory*, 7th edn.(McGraw-Hill, New York, 1979).
- [19] Khujadze, G. and Oberlack, M., “DNS and scaling laws from new symmetry groups of ZPG turbulent boundary layer flow,” Theoret. Comput. Fluid Dynamics, vol. 18, 2004, pp 391.
- [20] Falkner, V. and Skan, S., “Some Approximate solutions of the boundary layer solutions,” Philosophical Magazine, vol. 12, 865(1931).
- [21] Österlund, J., “Experimental studies of zero pressure-gradient turbulent boundary layer flow,” PhD thesis, Royal Institute of Technology, KTH, Stockholm, 1999.
- [22] Skåre, P.E. and Krogstad, P.A. “A Turbulent Equilibrium Boundary Layer near Separation,” J. Fluid Mech. Vol. 272, 319 (1994).
- [23] Clauser, F., “The turbulent boundary layer in adverse pressure gradients,” J. Aeronaut. Sci., vol. 21, 91 (1954). Data from Reference 24.
- [24] Coles, D., and Hirst, E., eds., *Proceedings of Computation of Turbulent Boundary Layers, AFOSR-IFP-Stanford Conference*, Vol. 2, (Thermosciences Div., Dept. of Mechanical Engineering, Stanford Univ. Press, Stanford, CA, 1969).
- [25] Herring, H. and Norbury, J., “Some Experiments on Equilibrium Boundary Layers in Favourable Pressure Gradients,” J. Fluid Mech. **27**, 541 (1967). Data from Reference 24.
- [26] Buschmann, M., and Gad-el-Hak, M., “Recent developments in scaling of wall-bounded flows,” Prog. Aerospace Sci., vol. 42, 419(2007).
- [27] Brzek, B., Turan, O., Anderson, C., and Castillo, L., “Outer Scaling in Turbulent Boundary Layers,” AIAA 2005-4814 (2005).

- [28] Townsend, A., *The Structure of Turbulent Shear Flow*, 2nd edn. (Cambridge University Press, Cambridge, 1956).
- [29] Castillo, L., and George, W., “Similarity Analysis for Turbulent Boundary Layer with Pressure Gradient: Outer Flow,” *AIAA J.*, vol. 39, 41(2001).
- [30] Cal, R, and Castillo, L., “Similarity analysis of favorable pressure gradient turbulent boundary layers with eventual quasilaminarization,” *Physics of Fluids*, vol. 20, 105106 (2008).
- [31] Maciel, Y., Rossignol, K.-S., and Lemay, J., “Self-Similarity in the Outer Region of Adverse-Pressure-Gradient Turbulent Boundary Layers,” *AIAA J.*, vol. 44, 2450 (2006).
- [32] Schubauer, G. and Klebanoff, P., “Investigation of Separation of the Turbulent Boundary Layer,” *NACA TN 2133* (1950). Data from Reference 24.
- [33] Sreenivasan, K., and Sahay, A., “The Persistence of Viscous Effects in the Overlap Region, and the Mean Velocity in Turbulent Pipe and Channel Flows,” *Self-Sustaining Mechanisms of Wall Turbulence*, ed. by R. Paton, Computational Mechanics Publications, Southhampton, UK, 1997, pp. 253-272.